Stem Cell Reports
Article

ISSCR

OPEN ACCESS

Dual Inhibition of GSK3β and CDK5 Protects the Cytoskeleton of Neurons from Neuroinflammatory-Mediated Degeneration *In Vitro* and *In Vivo*

Lydia Reinhardt,[1,2] Susanne Kordes,[2,3] Peter Reinhardt,[1,2,11] Michael Glatza,[1,2] Matthias Baumann,[3] Hannes C.A. Drexler,[4] Sascha Menninger,[3] Gunther Zischinsky,[3] Jan Eickhoff,[3] Claudia Fröb,[1] Prabesh Bhattarai,[1,5] Guruchandar Arulmozhivarman,[1] Lara Marrone,[1] Antje Janosch,[6] Kenjiro Adachi,[2] Martin Stehling,[2] Eric N. Anderson,[7,8] Masin Abo-Rady,[1] Marc Bickle,[6] Udai Bhan Pandey,[7,8,9] Michell M. Reimer,[1] Caghan Kizil,[1,5] Hans R. Schöler,[2,10] Peter Nussbaumer,[3] Bert Klebl,[3] and Jared L. Sterneckert[1,2,*]

[1]Technische Universität Dresden, DFG-Research Center for Regenerative Therapies Dresden (CRTD), Fetscherstrasse 105, 01307 Dresden, Germany
[2]Department of Cell and Developmental Biology, Max Planck Institute for Molecular Biomedicine, Röntgenstrasse 20, 48149 Münster, Germany
[3]Lead Discovery Center GmbH, Otto-Hahn-Strasse 15, 44227 Dortmund, Germany
[4]Bioanalytical Mass Spectrometry, Max Planck Institute for Molecular Biomedicine, Röntgenstrasse 20, 48149 Münster, Germany
[5]German Center for Neurodegenerative Diseases (DZNE) within the Helmholtz Association, Tatzberg 41, 01307 Dresden, Germany
[6]Max Planck Institute of Molecular Cell Biology and Genetics, 01307 Dresden, Germany
[7]Department of Pediatrics, Division of Child Neurology, Children's Hospital of Pittsburgh, University of Pittsburgh School of Medicine, Pittsburgh, PA 15224, USA
[8]Department of Human Genetics, University of Pittsburgh Graduate School of Public Health, Pittsburgh, PA 15261, USA
[9]Department of Neurology, University of Pittsburgh School of Medicine, Pittsburgh, PA 15213, USA
[10]University of Münster, Medical Faculty, Domagkstrasse 3, 48149 Münster, Germany
[11]Present address: AbbVie Deutschland GmbH & Co. KG, Neuroscience Discovery, Knollstrasse, 67061 Ludwigshafen, Germany
*Correspondence: jared.sterneckert@tu-dresden.de
https://doi.org/10.1016/j.stemcr.2019.01.015

SUMMARY

Neuroinflammation is a hallmark of neurological disorders and is accompanied by the production of neurotoxic agents such as nitric oxide. We used stem cell-based phenotypic screening and identified small molecules that directly protected neurons from neuroinflammation-induced degeneration. We demonstrate that inhibition of CDK5 is involved in, but not sufficient for, neuroprotection. Instead, additional inhibition of GSK3β is required to enhance the neuroprotective effects of CDK5 inhibition, which was confirmed using short hairpin RNA-mediated knockdown of CDK5 and GSK3β. Quantitative phosphoproteomics and high-content imaging demonstrate that neurite degeneration is mediated by aberrant phosphorylation of multiple microtubule-associated proteins. Finally, we show that our hit compound protects neurons *in vivo* in zebrafish models of motor neuron degeneration and Alzheimer's disease. Thus, we demonstrate an overlap of CDK5 and GSK3β in mediating the regulation of the neuronal cytoskeleton and that our hit compound LDC8 represents a promising starting point for neuroprotective drugs.

INTRODUCTION

As people live longer, the number of people suffering from neurological disorders, including neurodegenerative diseases, increases, and new treatments are urgently needed. Positron emission tomography studies demonstrate that neuroinflammation mediated by activated microglial cells is a common feature of patients diagnosed with many different neurodegenerative diseases, including amyotrophic lateral sclerosis (ALS) (Turner et al., 2004), Alzheimer's disease (AD) (Turner et al., 2004), and HIV-induced dementia (Vera et al., 2017), where activation correlates with disease severity. Consistent with this finding, neuroinflammation is associated with the production of agents such as nitric oxide (NO) that are neurotoxic. However, neuroinflammation can be beneficial as well, for example, by assisting in the clearance of protein aggregates and viral infections. Thus, therapeutics are needed that directly protect neurons from neuroinflammatory stress, ideally without suppressing neuroinflammation.

Phenotypic drug discovery is a powerful tool for the discovery of first-in-class drugs with new molecular mechanisms of action, and stem cells are ideal for generating disease models for use in phenotypic screenings because they provide theoretically limitless quantities of the neurons affected in patients. Previously, we reported the generation of a high-throughput screening assay using a stem cell-based model of neurodegeneration induced by neuroinflammation (Höing et al., 2012). Here, we report the results of a stem cell-based phenotypic screening campaign using high-content imaging to measure the integrity of the neuronal network as a readout for motor neuron (MN) survival. We identified a series of pyrazolotriazines that cell-autonomously protect MNs against neuroinflammation. We found that our hit compounds inhibited cyclin-dependent kinase (CDK) activity, but we found no evidence of cell cycle re-entry. Instead, we propose an alternative mechanism of neuroprotection. We discovered that inhibition of CDK5 was involved in, but not sufficient to protect MNs from, degeneration. LDC8 was the most potent hit

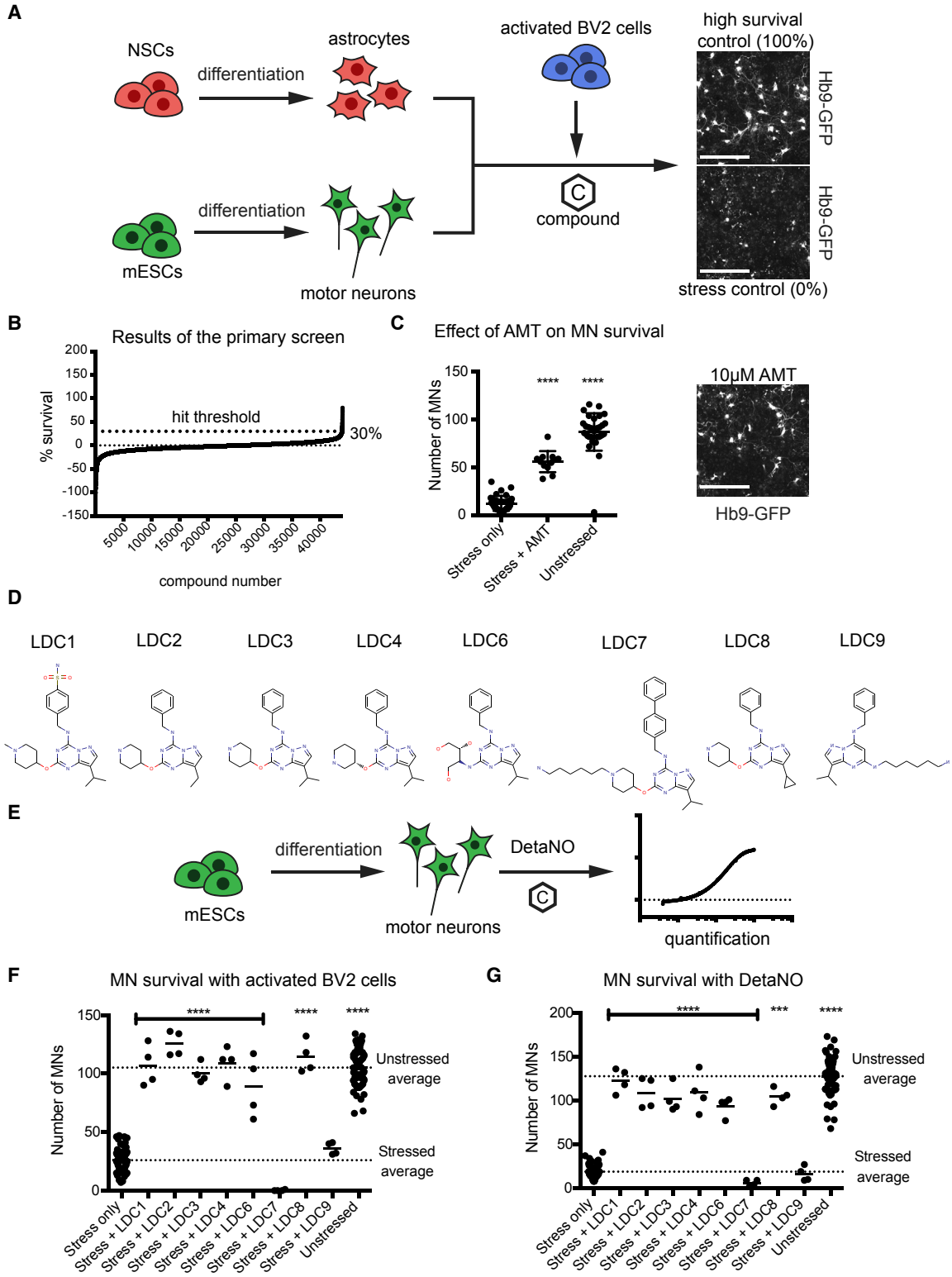

Figure 1. Identification of a Series of Hit Compounds Protecting Mouse MNs against Dying-Back Pathology Mediated by Stress-Induced Degeneration

(A) Schematic illustration of the assay design for the high-throughput screening campaign.

(legend continued on next page)

compound, which also inhibited glycogen synthase kinase 3β (GSK3β), and inhibition of GSK3β significantly enhanced the neuroprotective properties of CDK5 inhibition in mouse pluripotent stem cell-derived MNs as well as in human induced pluripotent stem cell (iPSC)-derived MNs. Quantitative phosphoproteomics of human iPSC-derived MNs demonstrated that neuroinflammation-like stress was associated with altered phosphorylation of microtubule-associated proteins (MAPs), which significantly impaired the integrity of the neuronal cytoskeleton. Strikingly, this was rescued by small molecules inhibiting GSK3β and CDK5. Knockdown experiments confirmed that reducing GSK3β and CDK5 levels rescued neurodegeneration induced by neuroinflammation-like stress. Notably, reduction of either GSK3β or CDK5 alone was insufficient. Finally, we demonstrate that our compound is sufficient to protect MNs *in vivo* in zebrafish models of MN degeneration and AD. Importantly, we could show that synaptic degeneration is ameliorated *in vivo* without inhibiting neuroinflammation. Therefore, our results suggest that dual inhibition of CDK5 and GSK3β is a powerful approach to protect neuronal morphology against neuroinflammatory stress, which is a common feature of many neurodegenerative diseases. LDC8 represents a promising starting point for lead optimization for neuroprotective drugs, and our phosphoproteomics results suggest possible biomarkers of target engagement to facilitate efficacy testing *in vivo*.

RESULTS

Phenotypic Screening Identifies Compounds Protecting MNs from Inflammation in a Cell-Autonomous Manner

Phenotypic screening enables the identification of disease-modifying molecular pathways in an unbiased manner. Previously, we established a phenotypic screening assay modeling MN degeneration mediated by neuroinflammation (Höing et al., 2012). *Hb9-GFP*-positive MNs differentiated from mouse embryonic stem cells (ESCs) were co-cultured with astrocytes differentiated from neural stem cells (Figure 1A). Neuroinflammation was modeled by adding microglial BV2 cells, which were activated using lipopolysaccharide (LPS) and interferon-γ (IFN-γ). Neuronal morphology was quantified to assess MN survival. We screened 44,000 small molecules to identify compounds that protected MNs from neuroinflammation-induced degeneration (Figure 1B and Table S1). We identified a hit series consisting of seven pyrazolotriazines that protected MNs above a threshold of 30% (Figures 1B and 1D). Two structurally related pyrazolotriazines containing a hexylamine substitution did not protect MNs from BV2-induced degeneration (Figures 1D and 1F), but rather disrupted the interaction with the cellular target.

It is possible that the identified hit compounds protected MNs by directly modulating BV2 cells. Once activated, microglia cells express iNOS, resulting in the production of NO, which is neurotoxic. For example, inhibition of iNOS by the specific inhibitor 2-amino-5,6-dihydro-6-methyl-4*H*-1,3-thiazine (AMT) protected MNs from BV2-induced degeneration, with a half-maximal inhibitory concentration (IC_{50}) of about 1.7 μM (Figure 1C), demonstrating that NO is an important mediator of BV2 cell-induced MN degeneration. To test if our hit compounds directly protected MNs, mouse ESC-derived MNs and mouse neuron stem cell (NSC)-derived astrocytes were co-cultured in the presence of diethylenetriamine/NO adduct (DetaNO), which is a chemical donor of NO and can be used to mimic the activity of iNOS by releasing NO into the culture medium (Figure 1E). Strikingly, the identified series of seven hit pyrazolotriazines protected MNs from DetaNO-mediated stress with comparable IC_{50} values of 2–6 μM (Figures 1F, 1G, and S1), suggesting that those compounds act directly on MNs. Consistent with the results from the original assay using BV2 cells, the two compounds

(B) Primary screening results of about 44,000 compounds. MN survival was defined as total neurite length normalized to high- and low-survival controls. A threshold of 30% was used to define active compounds.
(C) Inhibition of iNOS activity by AMT rescued mESC-derived MNs from BV2-induced degeneration. Bars indicate mean and SD for n = 8 independent observations using at least 1 μM AMT and n = 32 independent observations for controls.
(D) Chemical structures of the identified hit series.
(E) Schematic illustration of the assay to test if a compound directly rescues MNs from DetaNO-induced degeneration. DetaNO is a chemical donor of nitric oxide, which mimics activated microglial cells.
(F and G) The effectiveness of our hit compounds in rescuing MNs from activated microglia (BV2 cells) and DetaNO-induced degeneration is shown in (F) and (G), respectively. NSCs, neuron stem cells; mESCs, mouse embryonic stem cells. Bar indicates the mean. Each hit compound was tested at 6.7 and 20 μM, which was previously determined to the plateau phase of each compound using dose-response curves (data not shown), to give n = 4 independent replicates and compared with controls tested using n = 64 independent replicates. Dotted lines indicate the mean of the positive and negative controls. Ordinary one-way ANOVA was performed; ***p < 0.001 and ****p < 0.0001 compared with stress-only control according to Dunnett's multiple comparisons test.
See also Figure S1 and Table S1.

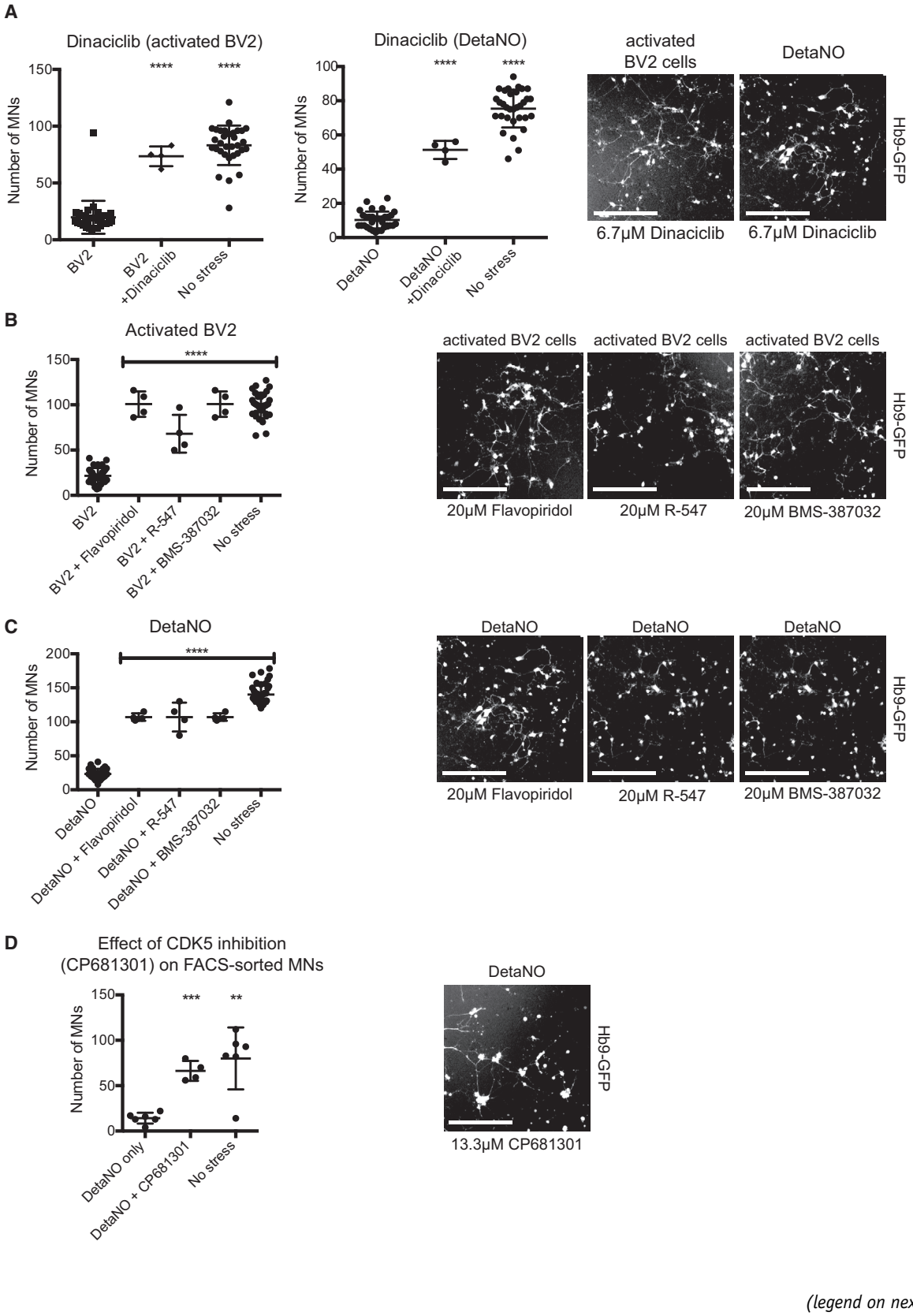

(legend on next page)

with a hexylamine substitution did not protect MNs from DetaNO-induced degeneration (Figure 1G). Interestingly, the small molecule LDC8 was the most effective compound in the series of hit compounds.

CDK Inhibitors Protect MNs from Inflammation-Mediated Degeneration

A chemical similarity search using PubChem suggested CDKs as potential targets of the active small molecule hits, but not of the inactive compounds. As such, we speculated that CDK inhibition protects MNs against neurodegeneration, and we tested the effects of several structurally distinct CDK inhibitors, including dinaciclib, BMS-387032, flavopiridol, and R-547, each of which inhibits a broad range of cellular CDKs. We found that all four structurally distinct CDK inhibitors robustly protected mouse ESC-derived MNs from degeneration induced by activated BV2 cells as well as by DetaNO (Figures 2A–2C). Taken together, these results demonstrate that several CDK inhibitors recapitulate the neuroprotective effects of our original hit compounds, suggesting that CDK inhibition might be a potential therapeutic approach.

Our hit compounds, as well as structurally unrelated CDK inhibitors, protect MNs from DetaNO-mediated inflammation-like stress in the absence of BV2 cells. Subsequently, we assessed if CDK inhibitors protected MNs via non-cell-autonomous mechanisms mediated by co-cultured astrocytes. In addition to supporting MNs with trophic factors, astrocytes are activated by LPS and IFN-γ, similar to microglial cells, leading to the secretion of factors that are toxic to co-cultured MNs (Höing et al., 2012). To further rule out non-cell-autonomous mechanisms mediated by astrocytes, mouse ESC-derived MNs were purified using fluorescence-activated cell sorting (FACS) and cultured in the presence of DetaNO, but in the absence of astrocytes. Consistent with previous results, we found that the pan-CDK inhibitor dinaciclib protected purified MNs from DetaNO-induced degeneration (Figure S2A). Therefore, we conclude that CDK inhibitors directly protect MNs from inflammation-mediated degeneration induced by activated BV2 cells or DetaNO.

CDK5-Specific Inhibitor CP681301 Protects Mouse and Human MNs from Degeneration

The neuroprotective compounds tested above inhibit multiple CDK proteins simultaneously. To determine the specific molecular target of our active hit compounds, we profiled the ability of our hit compounds to inhibit the biochemical activity of a panel of purified CDKs, including CDK1, CDK2, CDK4, CDK5, CDK6, CDK7, and CDK9 (Table S2). During target deconvolution, we found that one of our hit compounds, LDC9, inhibited CDK7 and CDK9, but did not rescue MNs from DetaNO-induced degeneration (Figure S2B), suggesting that neither of these CDKs is involved in neuroprotection. PD332991 is known to inhibit CDK4 and CDK6, and, in addition, KINOMEscan profiling (Fabian et al., 2005) shows that PD332991 significantly reduces ATP binding to CDK7 and CDK9 at a concentration of 10 μM (http://lincs.hms.harvard.edu/db/datasets/20044/), suggesting it inhibits CDK7 and CDK9 as well. However, when tested in our assay, PD332991 was not neuroprotective, even when tested at concentrations larger than 10 μM (Figure S2C), indicating that CDKs 4, 6, 7, and 9 are not involved in neuroprotection. Because the expression levels of CDK1 in FACS-purified mouse MNs were below 100 arbitrary units (Table S3), which was our threshold for expressed genes, inhibition of CDK1 is also not likely to mediate neuroprotection. In addition, when we tested the CDK1/2-specific inhibitor NU6102 in our assay, it was not protective (Figure S2D). Taken together, these data demonstrate that inhibition of CDK1, CDK2, CDK4, CDK6, CDK7, or CDK9 individually is not sufficient to protect MNs from NO-induced degeneration.

CDK5 activity is neuron specific and involved in neuronal development, synaptic plasticity, and phosphorylation of cytoskeletal proteins (Kawauchi, 2014). Interestingly, aberrant activation of CDK5 has been shown to contribute to AD pathology (Shukla et al., 2013; Zheng et al., 2010). Because dinaciclib inhibits CDK5 activity as well as canonical cell-cycle-associated CDKs, we speculated that dinaciclib might protect mouse MNs from inflammation-induced degeneration by inhibiting CDK5. To test our hypothesis that CDK5 inhibition protects MNs from

Figure 2. Pan-CDK Inhibitors Protect Mouse MNs against Stress-Induced Degeneration

(A–C) (A) Dinaciclib rescued mouse ESC-derived MNs from activated neuroinflammatory stress mediated by microglia (BV2 cells) or a chemical donor of NO (DetaNO). The CDK inhibitors flavopiridol, R-547, and BMS-387032 rescued mouse ESC-derived MNs from (B) activated neuroinflammatory stress mediated by microglia (BV2 cells) or (C) a chemical donor of NO (DetaNO). Fluorescence micrographs of *Hb9*-GFP-positive MNs illustrate the integrity of the neuronal network.

(D) Specific inhibition of CDK5 using CP681301 effectively protects mouse ESC-derived MNs from DetaNO-induced neurodegeneration. Dotted line indicates average of unstressed and stress-only controls. Bars indicate the mean. Each compound was tested using n = 4 replicates and controls were tested using n = 32 (A–C) or n = 6 (D) independent replicates. Bars indicate mean and SD.

Ordinary one-way ANOVA was performed; **p < 0.01, ***p < 0.001, and ****p < 0.0001 compared with stress-only control according to Dunnett's multiple comparisons test. See also Figure S2 as well as Tables S2, S3, and S4.

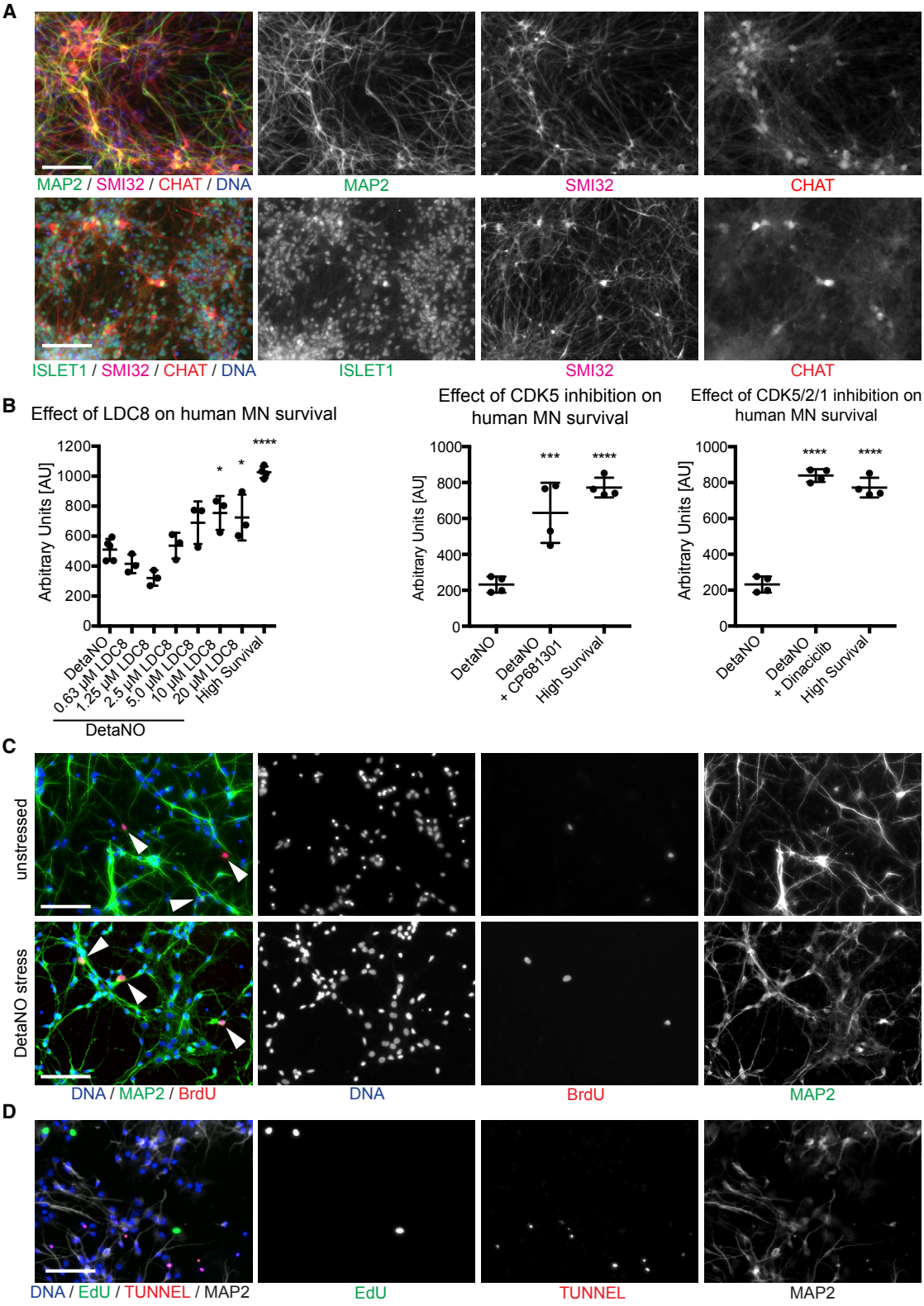

(legend on next page)

stress-induced degeneration, we used the CDK5-specific inhibitor CP681301 on FACS-purified MNs cultured in the presence of DetaNO. Strikingly, we observed a dose-dependent rescue effect (Figure 2D), suggesting that inhibition of CDK5 could contribute to MN protection in our assay.

Although mouse ESC-derived MNs represent a powerful tool for high-throughput screenings, species-specific differences between mice and humans might lead to the identification of false positive targets. To investigate if CDK inhibition also rescues human MNs from inflammation-induced degeneration, we used human iPSCs from healthy donors and differentiated them via expandable neural progenitor cells (NPCs) into MNs (Reinhardt et al., 2013). When exposed to MN differentiation and maturation medium for 21 days, NPCs efficiently formed MAP2, SMI32, and ChAT triple-positive cells, which are markers of MN identity (Figure 3A). Immunostaining demonstrated the presence of SMI32 and ChAT double-positive cells that also express ISLET1, which further confirmed the MN identity of these cells (Figure 3A). To test the neuroprotective effect of CDK inhibition on human iPSC-derived neurons, differentiated MNs were exposed to 400 μM DetaNO in the presence of the pan-CDK inhibitor dinaciclib. To measure cellular viability, we used CellTiter-Glo, which quantifies ATP levels. Consistent with our previous results using mouse ESC-derived MNs, dinaciclib potently rescued human MNs from neuroinflammation-like stress (Figure 3B). Subsequently, we also tested our hit compound LDC8 as well as the CDK5 inhibitor CP681301 on human iPSC-derived MNs in the presence of DetaNO. Strikingly, both compounds rescued human MNs from stress-induced degeneration, which is consistent with our previous results using mouse MNs (Figure 3B), suggesting that aberrant CDK5 activity mediates inflammation-induced MN degeneration.

Aberrant cell cycle re-entry of post-mitotic neurons mediated by CDK activity has been suggested to contribute to neurodegeneration. MNs in ALS patients as well as cortical neurons in Alzheimer patients have been shown to express aberrant cell cycle markers, and CDK inhibitors protected iPSC-derived neurons from amyloid-induced neurodegeneration (Xu et al., 2013). However, our data showed that canonical cell cycle CDKs played little or no role in MN protection, suggesting that MN degeneration is independent of cell cycle re-entry. To test if MNs undergo aberrant cell cycle re-entry under stressed conditions, we performed a bromodeoxyuridine (BrdU) incorporation experiment using cultures of differentiated human iPSC-derived MNs in the presence and absence of DetaNO followed by immunofluorescence for BrdU and MAP2. Interestingly, we detected BrdU-positive cells that expressed the neuronal marker MAP2. However, the numbers of BrdU-positive cells represented only a minority of all cells and were similar between stressed and unstressed conditions, suggesting that DetaNO-induced neurodegeneration is not mediated by aberrant cell cycle re-entry (Figure 3C). This result was corroborated by the absence of 5-ethynyl-2′-deoxyuridine (EdU) and TUNEL double-positive neurons, which would indicate apoptotic cells re-entering the cell cycle, in the presence of stress (Figure 3D). Taken together, these results demonstrate that stress-induced neurodegeneration in human MNs occurs independent of S-phase entry in our system.

Knocking Out CDK5 Is Not Sufficient to Ameliorate Stress-Induced MN Degeneration

Since small-molecule kinase inhibitors often exhibit off-target effects on structurally related proteins, we next used a genetics-based approach to test if CDK5 inhibition was sufficient to protect MNs from stress-induced degeneration. Using CRISPR/Cas9-mediated gene editing we knocked out the *CDK5* locus in mouse ESCs carrying the *Hb9-GFP* transgene (Figure 4A). DNA sequencing, and western blotting confirmed the absence of CDK5 protein in multiple clonal lines (Figures 4A and 4C). FACS sorting for GFP-positive MNs demonstrated that knocking out

Figure 3. CDK Inhibitors Protect Human iPSC-Derived MNs from Neuroinflammation-like Degeneration Independent of Cell Cycle Re-entry

(A) Immunostaining of human MNs for the indicated markers. MNs were differentiated from iPSCs via a small-molecule expandable neural progenitor cell intermediate.

(B) CellTiter-Glo assay results for human MNs stressed with 400 μM DetaNO in the presence of the indicated concentrations of LDC8 (n = 3 independent replicates), CP681301 (CDK5 inhibitor at a concentration of 2–6 μM; n = 4 independent replicates), or dinaciclib (CDK5/2/1 inhibitor at a concentration of 0.1–0.3 μM; n = 4 independent replicates). The results for unstressed MNs are shown for comparison. Ordinary one-way ANOVA was performed; *p < 0.05, ***p < 0.001, and ****p < 0.0001 compared with stress-only control according to Dunnett's multiple comparisons test.

(C) Immunostaining demonstrated that differentiated human MNs rarely incorporated BrdU, a marker for S phase, indicated by arrowheads. DetaNO (400 μM) had no significant effect on the number of neurons positive for BrdU, suggesting that cell cycle re-entry played little, if any, role in the observed MN degeneration.

(D) When treated with DetaNO, TUNEL-positive human MNs were not positive for EdU, a marker of S phase, consistent with the observation that cell cycle re-entry plays no role in MN degeneration induced by DetaNO. Scale bar, 100 μm.

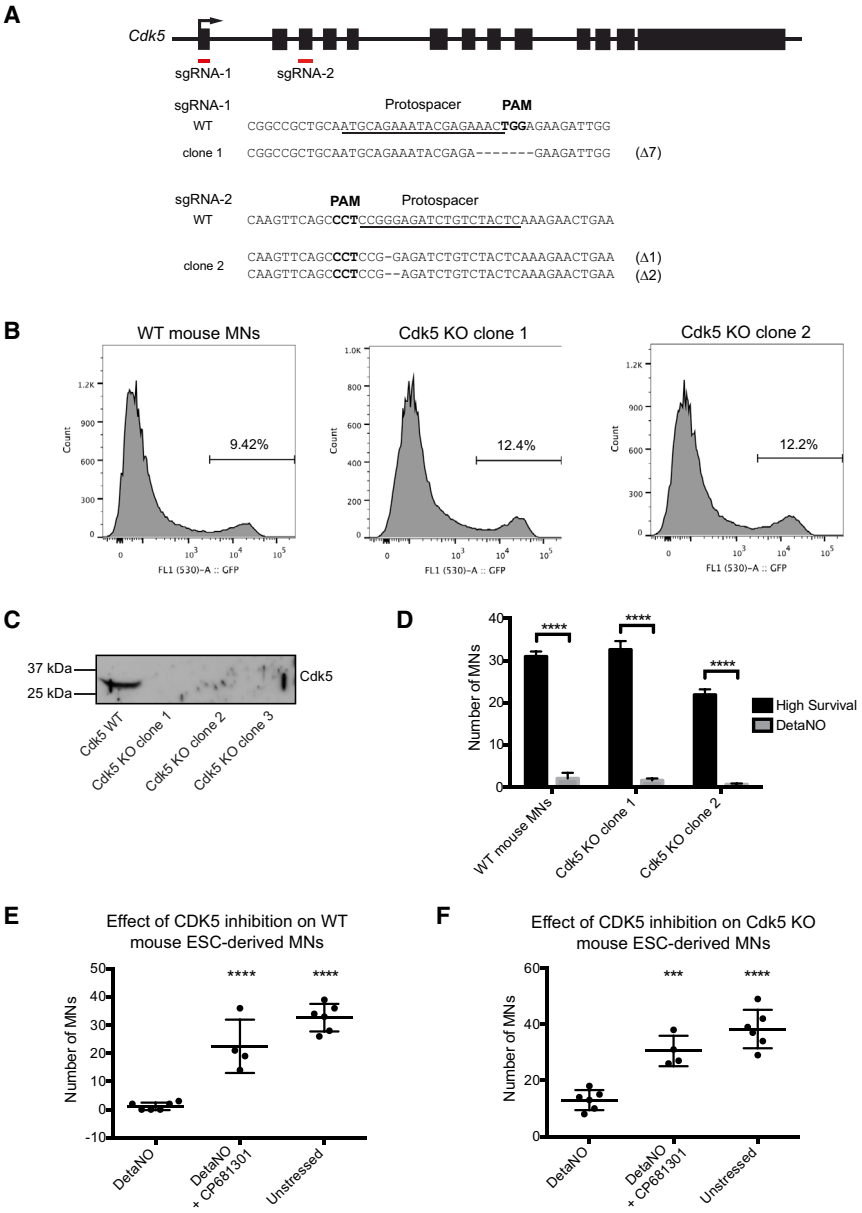

Figure 4. Knockout of Cdk5 Is Not Sufficient to Protect Mouse MNs from DetaNO-Induced Degeneration

(A–C) (A) Strategy that was used to knock out Cdk5 in mESCs. Locations of single guide RNAs (sgRNAs) used for CRISPR/Cas9-mediated gene editing are indicated. Validation of knockout using Sanger sequencing and western blot analysis is shown in (B) and (C), respectively.

(D) Flow cytometry demonstrates that removal of Cdk5 had no effect on MN differentiation efficiency (n = 20). ****p < 0.0001 according to t test.

(E and F) DetaNO-induced degeneration of MNs (E) with Cdk5 and (F) with a Cdk5 knockout. CP681301 was tested at 20 and 40 μM using n = 4 independent replicates. Positive and negative controls were performed in n = 6 independent replicates. Bars indicate mean and SD.

Ordinary one-way ANOVA was performed; ***p < 0.001 and ****p < 0.0001 compared with DetaNO alone calculated using Dunnett's multiple comparison's test. See also Figure S3.

CDK5 had no effect on MN differentiation efficiency of several clones (Figure 4B). If our hypothesis is correct that inhibition of CDK5 protects MNs from stress-induced degeneration, then MNs differentiated from mouse ESC-derived MNs lacking CDK5 should be resistant to degeneration induced by DetaNO (Figure 4D). However, we found that MNs with and without CDK5 degenerated in comparable manners when cultured in the presence of DetaNO. Taken together, these data demonstrate that reducing CDK5 activity is not sufficient to protect MNs from degeneration induced by inflammatory stress, suggesting that at least one additional target is required for effective neuroprotection.

Since the CDK5-specific inhibitor CP681301, as well as our hit compounds, protected MNs from neuroinflammatory stress, we speculated that CP681301 as well as our primary hits was inhibiting a second kinase, in addition to CDK5, to mediate neuroprotection. To test this, we stressed mouse MNs lacking *Cdk5* with DetaNO in the presence of increasing concentrations of CP681301 and compared their response with that of the respective parental wild-type (WT) controls (Figures 4E and 4F). Consistent with our hypothesis, CP681301 had similar effects on WT and CDK5 knockout (KO) MNs, indicating that at least one additional target is required for effective neuroprotection.

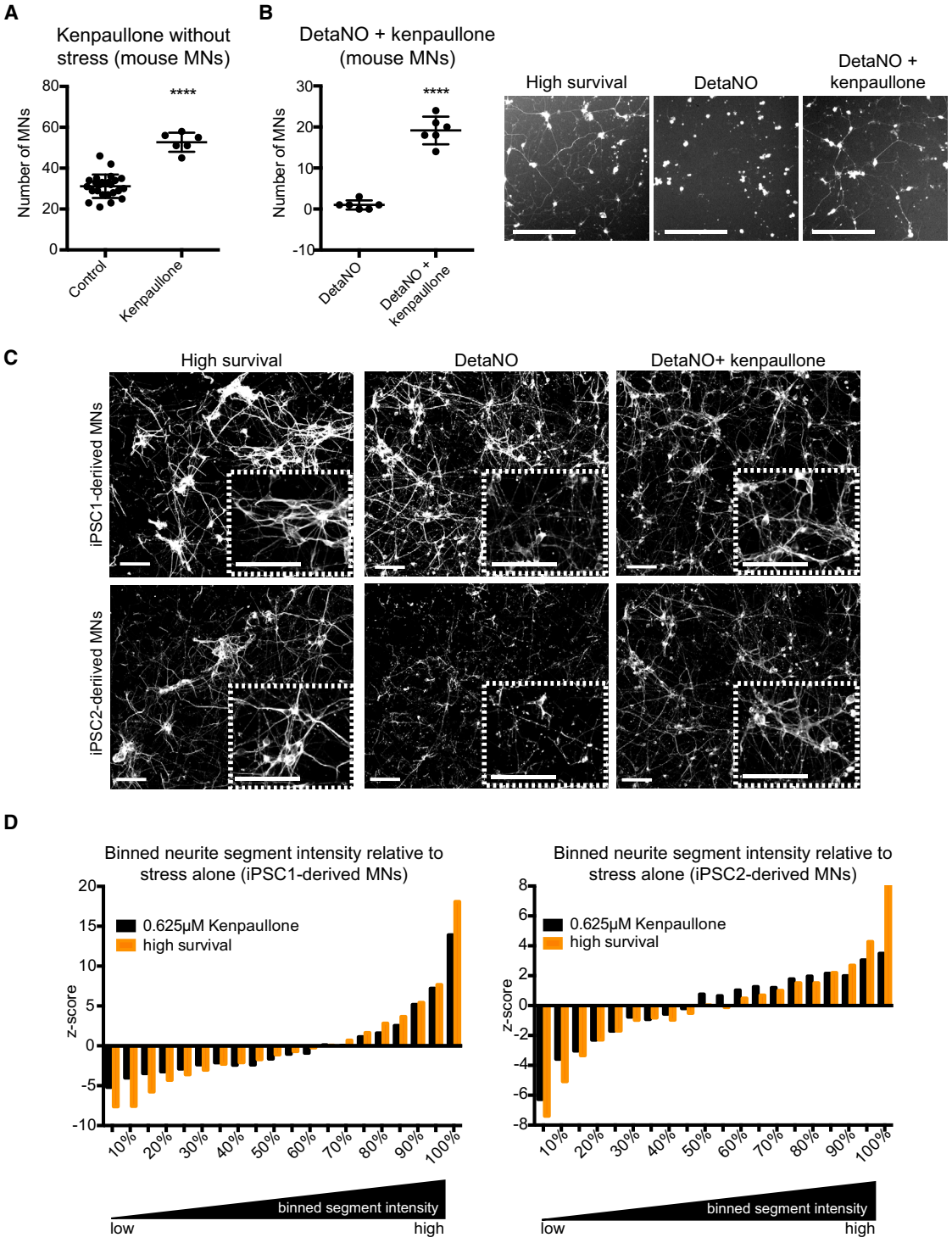

Figure 5. Dual Inhibition of CDK5 and GSK3β by Kenpaullone Protects Mouse and Human MNs from DetaNO-Induced Degeneration

(A) Unstressed *Hb9*-GFP mouse ESC-derived MNs treated with 10–40 μM kenpaullone using n = 6 independent replicates with controls having n = 24 independent replicates. Bars indicate mean and SD. ****p < 0.0001 according to t test.

(B) *Hb9*-GFP mouse ESC-derived MNs were treated with DetaNO and kenpaullone as well as controls having n = 6 independent replicates. Representative images show 10 μM kenpaullone. ****p < 0.0001 according to t test. Bars indicate mean and SD.

(legend continued on next page)

Inhibition of GSK3β Contributes to MN Protection

We speculated that CDK inhibitors that rescued MNs from inflammation-like stress required inhibition of more than one kinase. Since CDK proteins are closely related, many CDK inhibitors target multiple CDKs simultaneously, which is often associated with toxicity. To explore this issue more closely, we cultured mouse ESC-derived MNs with increasing concentrations of a CDK inhibitor in the absence of any stress. We consistently observed that dinaciclib, BMS-387302, flavopiridol, R547, LDC1, LDC2, LDC4, and CP681301 induced toxicity at at least one tested concentration (Figures S3A and S3B and Table S4), which was rescued by further increasing the concentration. As the CDK5-KO MNs resembled WT MNs, the toxicity and rescue are likely due to additional kinases being inhibited. Thus, we suggest that there are at least two targets in addition to CDK5: one that is toxic when inhibited and another that is protective when inhibited.

To identify which kinase, in addition to CDK5, is targeted by our hit compounds we used publicly available KINOMEscan data, which profile the ability of a compound to compete with over 400 individual kinases and prevent their binding to an ATP-like ligand. Interestingly, we found that the pan-CDK inhibitors BMS-387032 (http://lincs.hms.harvard.edu/db/datasets/20171/) and flavopiridol (http://lincs.hms.harvard.edu/db/datasets/20193/) bind GSK3β with high affinity (low K_d) and potently inhibit GSK3β activity. Similarly, 1 μM dinaciclib reduced the activity of GSK3β by about 70% in a biochemical assay (Chen et al., 2016). Consistent with these observations, biochemical assays demonstrated that LDC8, which exhibited the most potent neuroprotection of our hit compounds, inhibited GSK3β with an IC_{50} of 1.4 μM. Since experiments have demonstrated that GSK3β activity contributes to AD (Kremer et al., 2011) and ALS (Koh et al., 2007), we speculated that our identified compounds protect MNs via simultaneous inhibition of GSK3β and CDK5.

To test if GSK3β is required to mediate neuroprotection, we tested whether CHIR99021 (hereafter abbreviated CHIR), which is a specific GSK3β inhibitor, would rescue MNs from the cytotoxic effects observed with CDK inhibitors. Mouse MNs were incubated with 5 μM CP681301 in the presence of increasing concentrations of CHIR. Significantly, we found that CHIR rescued MNs from CP681301-mediated cytotoxicity (Figure S3C). In addition, CHIR did not show any cytotoxic effects (Figure S3D) as observed with the tested CDK inhibitors. We even found that CHIR induced a small, but significant increase in the survival and neurite morphology of ESC-derived MNs under unstressed conditions. In contrast, when we tested if CHIR alone is sufficient to rescue MNs from DetaNO-induced degeneration, GSK3β inhibition failed to protect mouse MNs (Figure S3E). Interestingly, similar results were obtained when human iPSC-derived MNs were treated with CHIR in the presence of the neuroinflammatory stressor DetaNO (Figures S3F and S4). These data indicate that specific inhibition of CDK5 and GSK3β would protect MNs. To test this, we used kenpaullone, which specifically inhibits CDK5 and GSK3β. Consistent with our hypothesis, we found that kenpaullone robustly protected mouse and human MNs from degeneration induced by DetaNO (Figures 5B–5D and S5), reinforcing the idea that our hit compounds protect from inflammation-like stress by inhibiting CDK5 and GSK3β.

Subsequently, we used a knockdown approach to further validate that reduction of CDK5 and GSK3β was sufficient to protect MNs from degeneration. Lentiviral expression vectors were used to deliver short hairpin RNA (shRNA)-mediated knockdown of CDK5 and GSK3β in human iPSC-derived MNs. Western blot analysis confirmed that CDK5 and GSK3β proteins were reduced compared with MNs that were infected with scrambled control shRNAs (Figure S6). Human iPSC-derived MNs that were cultured in the presence of DetaNO showed significantly greater levels of ATP, which marks survival, compared with scrambled controls as well as cultures in which *CDK5* and *GSK3β* were reduced individually (Figure S6). Thus, we conclude that reduction of *CDK5* and *GSK3β* is sufficient to protect human MNs against inflammatory-like conditions.

Finally, we sought to identify the off-target kinase(s) mediating the degeneration observed at lower concentrations of our hit compounds. To do this, we re-examined the results of our primary screening assay. Many of the compounds we found in our original screen protected neurons by killing BV2 cells, but because we were interested in compounds that directly protect MNs, these compounds were filtered out and not pursued. However, at least one of these rejected compounds, which we named LDC10, was structurally similar to our original hit series. In contrast to our hit compounds, which act directly on MNs, LDC10 rescued mouse ESC-derived MNs by killing co-cultured BV2 cells and was not able to protect MNs

(C) MNs differentiated from two different iPSC lines were treated with 400 μM DetaNO and 0.625 μM kenpaullone. Unstressed cultures were included as controls. Cultures were immunostained for TUBB3, and neurites were segmented between cross points using CellProfiler. Dashed boxes show a magnified portion of the image.

(D) Histograms for *Z* score resulting from n = 4 independent replicates of neurite segment area, demonstrating that kenpaullone and unstressed neurons have increased numbers of large area segments and reduced short segments. *Z* score of ±1.96 equals p value of 0.05. Scale bar, 100 μm. See also Figures S4–S6.

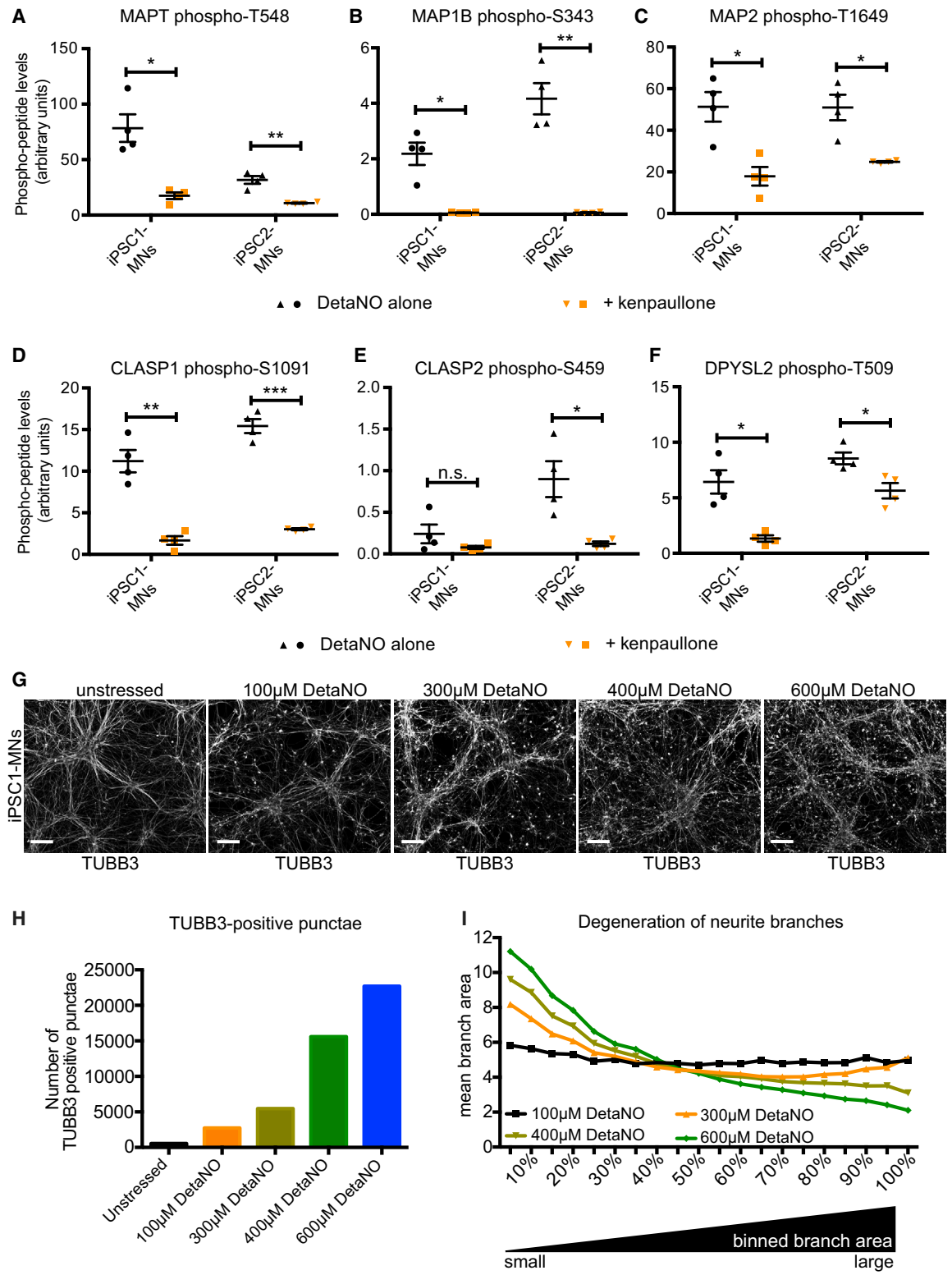

Figure 6. Kenpaullone Inhibits the Phosphorylation of Several Proteins Regulating Neuronal Microtubule Networks

(A–F) Label-free quantitative (LFQ) phosphoproteomics was performed using DetaNO-treated MNs from two different iPSC lines (iPSC1 and iPSC2) with and without kenpaullone. (A) MAPT phospho-T548; (B) MAP1B phospho-S343; (C) MAP2 phospho-T1649; (D) CLASP1

(legend continued on next page)

from DetaNO-induced degeneration (Table S4). This clearly suggested that toxicity was part of its mechanism. Significantly, LDC10 is structurally related to our hit compounds, suggesting that identification of the targets of LDC10 would also reveal off-targets of our hit compounds that mediate toxicity. Biochemical profiling demonstrated that LDC10 efficiently and specifically inhibited CDK7 (Table S2), suggesting that CDK7 is required for survival. CDK7 and CDK9 are required for transcription, which is essential for viability. All of the tested CDK inhibitors, including LDC8, efficiently inhibited CDK7 and/or CDK9 except kenpaullone (Table S2). Significantly, we found that kenpaullone showed no visible toxicity to mouse MNs, but, instead, mediated a small increase in MN survival (Figure 5A). We conclude that our hit compounds protect from inflammation-like stress by inhibiting CDK5 and GSK3β, and future lead optimization aimed at reducing inhibition of CDK7 and CDK9 by our hit compounds would be needed to reduce non-specific toxicity under unstressed conditions.

Phosphoproteomics Links CDK5 and GSK3β-Mediated Neuroprotection to Cytoskeletal Dynamics

To further investigate the molecular mechanism by which our hit compounds protect MNs, we used label-free quantitative phosphoproteomics on iPSC-derived MNs that were treated with DetaNO in the presence and absence of LDC8, which was our most potent hit compound. Gene ontology (GO) analysis revealed that microtubule cytoskeleton organization was significantly enriched, with a p value of about 1.5×10^{-6} (Table S5). However, many additional terms were related to RNA transcription and splicing, which are known to be regulated by CDK7 and CDK9. Because CDK7 and CDK9 represent off-targets of LDC8 that have been associated with toxicity, we repeated the phosphoproteomics experiment using kenpaullone, which does not inhibit CDK7 or CDK9. We identified 48 different phosphopeptides in 41 different proteins that were significantly decreased in the presence of kenpaullone compared with the stressed-only controls (Table S5). Twenty-six of 48 phosphopeptides contained a GSK3β substrate motif, and 22 phosphopeptides contained a CDK5 substrate motif. Significantly, all 22 peptides containing a CDK5 substrate motif were also predicted to be targets of GSK3β, indicating a substantial substrate overlap (Table S5). These results are consistent with our observation that dual inhibition of GSK3β and CDK5 is essential for efficient neuroprotection.

GO analysis revealed that microtubule organization and negative regulation of microtubule depolymerization (both with p value of about 2.6×10^{-8}; Table S4) were the most significantly regulated processes affected by kenpaullone-mediated inhibition of GSK3β and CDK5, both of which had a p value of about 2.6×10^{-8} (Table S5). Interestingly, additional GO terms directly related to microtubule organization were also affected by kenpaullone (Table S5). MAPs, such as MAPT (also known as TAU), MAP1B, and MAP2, were prominently represented in the GO term analysis, and phosphopeptide levels were consistently decreased by kenpaullone (Figures 6A–6C and Table S5). In addition, kenpaullone reduced the phosphorylation levels of CLASP1, CLASP2, and DPYSL2 (also known as CRMP2) compared with MNs that had been cultured in the presence of DetaNO (Figures 6D–6F). This is particularly interesting because CLASPs and DPYSL2 are MAPs that specifically regulate the dynamics of microtubules and hence suppress microtubule disassembly. Increased phosphorylation of MAPs, including MAPT, MAP2, CLASPs, and DPYSL2, enhances microtubule instability and disassembly, axonal trafficking defects, and neurodegeneration (Alonso et al., 1997). In contrast to the phosphoproteomics results for LDC8 above, the phosphoproteomics results for kenpaullone did not show GO-term enrichment for RNA-related splicing or processing, which is consistent with these being the results of non-specific inhibition of CDK7 and/or CDK9.

Microtubules are integral components of the cytoskeleton and organize the highly polarized structure of neurons. Therefore, alterations in microtubule dynamics can have large effects on neuronal morphology. For these reasons, we speculated that microtubules undergo catastrophe and depolymerization in neurons treated with DetaNO, potentially resulting in neurite swellings, which could manifest as punctate staining of β3-tubulin (TUBB3), which is neuron specific, instead of smooth and evenly distributed TUBB3 staining of microtubules in healthy neurites, which were segmented between cross points and quantified. To validate that NO induces microtubule defects in MNs, iPSC-derived MNs were treated with 400 μM DetaNO for 24 h and immunostained for TUBB3. We observed a large increase in the number of TUBB3-positive punctae (Figures 6G and 6H), consistent with the

phospho-S1091; (E) CLASP2 phospho-S459; (F) DPYSL2 phospho-T509. Linear values were derived from LFQ for the indicated phosphopeptide. Plots show means of LFQ values and error bars represent SEM, n = 4 replicates. *p < 0.05, **p < 0.01, and ***p < 0.001.
(G–I) (G) iPSC-derived MNs were treated with the indicated concentrations of DetaNO followed by immunostaining for TUBB3 to illustrate microtubule degeneration in the presence of stress. Images were segmented and quantified for TUBB3-positive punctae as an indicator for a disrupted tubulin network (H) as well as the neurite segment area histogram in (I).
Scale bar, 100 μm. See also Table S5.

hypothesis that DetaNO induces microtubule alterations. Next, we tested if this effect was dose dependent. As expected, increasing concentrations of DetaNO induced an almost linear increase in the number of TUBB3-positive punctae (Figure 6H). Consistent with previous results, DetaNO decreased the area of TUBB3-positive neurite segments (Figure 6I). These results demonstrate that NO, one of the major secreted factors of activated microglia, significantly alters the microtubule network in neurons, consistent with the phosphoproteomic data, and that kenpaullone prevents misregulation resulting in axonal degeneration by inhibiting CDK5 and GSK3β.

LDC8 Protects MNs against Degeneration *In Vivo*

We used a transgenic zebrafish model to test the efficacy of our hit compound to protect neurons *in vivo*. Since degeneration of oligodendrocytes precedes neuroinflammation and neurodegeneration in ALS (Kang et al., 2013), we speculated that depletion of oligodendrocytes plays a critical role in initiating subsequent neuroinflammation and neurodegeneration. To model this, we specifically depleted oligodendrocytes in larval zebrafish. To achieve this, a double transgenic line Tg(ClaudinK:Gal4 × UAS:nfsB-mCherry) was generated, which allows genetic ablation of mature oligodendrocytes and Schwann cells using the nitroreductase system (Figure S7A). nfsB-mCherry fusion protein converts the harmless prodrug metronidazole into a toxin (Knox et al., 1988). nfsB-mCherry is driven by ClaudinK:Gal4, which is specifically expressed in myelinating cells (Munzel et al., 2012). Thus, metronidazole specifically depletes myelinating cells in fish with Tg(ClaudinK:Gal4 × UAS:nfsB-mCherry). Metronidazole treatment was associated with a significant increase in the number of MPO:eGFP-positive neutrophils in fish compared with controls, consistent with a significant increase in inflammation (Figures S7B and S7C). An Hb9-GFP reporter was used to count MNs, revealing that depletion of oligodendrocytes results in a loss of about 20% of MNs in the spinal cord.

Subsequently, we tested the ability of LDC8 to protect MNs against degeneration induced by oligodendrocyte depletion. Tg(ClaudinK:Gal4 × UAS:nfsB-mCherry) fish with Hb9-GFP were treated with metronidazole in the presence of increasing concentrations of LDC8. DMSO was used as a negative control. In two different experiments, we observed a statistically significant rescue of Hb9-GFP-positive MNs (Figures S7D and S7E). As expected, LDC8 exhibited toxicity at higher concentrations, which is consistent with our earlier observations using human and mouse neurons and is due to inhibition of off-target proteins such as CDK7 and CDK9. We conclude that LDC8, which inhibits GSK3β and CDK5, protects MNs against degeneration *in vivo*.

LDC8 Increases Synaptic Density in an Adult Zebrafish AD Model

Finally, we tested whether LDC8 would be effective in preventing synaptic degeneration during AD pathogenesis using an established adult zebrafish amyloidosis model showing AD-like symptoms, including inflammation and synaptic degeneration (Bhattarai et al., 2016, 2017a, 2017b). Amyloid-β42 (Aβ42), which plays a critical role in AD, was microinjected cerebroventricularly into adult zebrafish brains either alone or in combination with LDC8 (Figure 7A). After 7 days, immunostaining was performed on tissue sections for L-plastin, which marks immune cells (Figures 7B and 7C), and synaptophysin, which marks synapses (Figures 7D and 7E). As expected, brains injected with Aβ42 showed elevated levels of immune cells in both activated (round) and resting (ramified) states compared with controls (Figures 7B and 7C). The number and morphology of immune cells was unchanged between Aβ42 alone and Aβ42 plus LDC8 (Figures 7B and 7C). Synaptic density in the zebrafish brain decreased by 68.4% at 7 days after injection with Aβ42 compared with vehicle (Figures 7D and 7E). LDC8 co-treatment with Aβ42 reduced synaptic density by 46.7% compared with vehicle, which is an increase of 67.6% compared with Aβ42 alone (Figure 7E). These results show that LDC8 significantly enhances synaptic survival in the presence of an inflammatory environment induced by Aβ42, which is a model of AD.

DISCUSSION

Neuroinflammation, including microglial activation, is a hallmark of many neurodegenerative disorders. Although neurotoxic agents such as NO are generated by activated microglial cells, they also assist in viral clearance and phagocytosis of protein aggregates. Thus, reduction of microglial activation using minocycline exacerbated ALS pathology in clinical trials (Gordon et al., 2007). For this reason, compounds are needed that protect neurons from degeneration until the underlying pathology has been cleared. Using phenotypic screening, we identified a small molecule, LDC8, that protects neurons, including their processes, from degeneration by inhibiting GSK3β as well as CDK5. Using shRNA-mediated knockdown in iPSC-derived neurons, we show that reduction of both GSK3β and CDK5 is neuroprotective. Importantly, we demonstrate that LDC8 protected against synaptic degeneration without disrupting neuroinflammation *in vivo*. Consistent with our results, previous studies have linked GSK3β and CDK5 to many neurodegenerative diseases, including ALS (Koh et al., 2007; Nguyen et al., 2001).

While previous reports show that CDK inhibitors, such as roscovitine and flavopiridol, protect neurons against

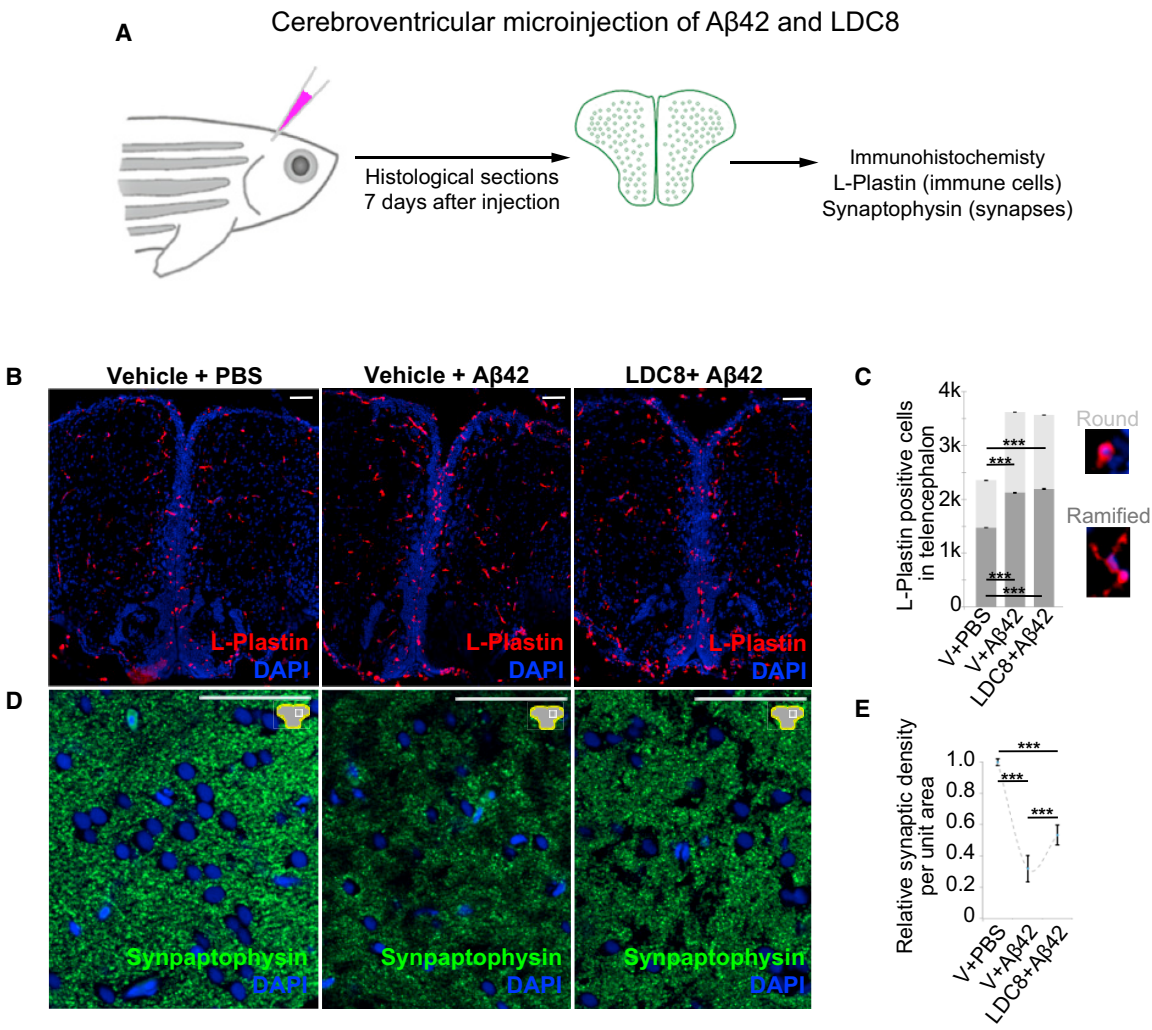

Figure 7. LDC8 Reduces the Synaptic Degeneration in an Adult AD Model in Zebrafish

(A) Graphic representation of the cerebroventricular microinjection and experimental scheme in adult zebrafish brain.

(B) Immunohistochemistry for L-plastin (immune cells) in fish brains injected with vehicle and PBS, vehicle and Aβ42, and LDC8 and Aβ42.

(C) Quantification graph for the numbers of active (round) and resting (ramified) immune cells after three injection conditions. Insets next to the graph indicate typical morphology.

(D) Immunohistochemistry for synaptophysin (synaptic connections) in fish brains injected with vehicle and PBS, vehicle and Aβ42, and LDC8 and Aβ42.

(E) Quantification graph for the relative synaptic density. Aβ42 significantly reduces the synaptic connections while LDC8 provides a significant increase in the surviving synapses. ***$p < 0.001$.

Scale bars, 50 μm. See also Figure S7.

diverse toxic agents (Rideout et al., 2003; Xu et al., 2013), we demonstrate an unexpected mechanism of neuroprotection by CDK inhibitors. As CDKs are well characterized for their role in regulation of the cell cycle, these reports have suggested that roscovitine and flavopiridol protect neurons by inhibiting cell cycle re-entry. In contrast, we found no evidence that inflammatory stress induces cell cycle re-entry. Rather, using phosphoproteomics, we demonstrate that dysregulation of the microtubules by aberrant GSK3β and CDK5-mediated phosphorylation of microtubule-binding proteins plays critical roles in degeneration-induced inflammation-like stress. Many of those phosphopeptides contain phosphorylation motifs for GSK3β and CDK5, suggesting that the phosphorylation event might be directly mediated by both GSK3β and CDK5. Consistent with this idea, CDK5 and GSK3β are both members of the CMPK kinase family and are structurally homologous. It is significant that mutations in

TUBA4A are associated with familial ALS, corroborating the idea that cytoskeletal defects cause neurodegeneration (Smith et al., 2014). Interestingly, inhibition of GSK3β was previously shown to protect MNs by stimulating autophagy *in vivo* in a mouse model treated with a toxin (de Munck et al., 2016). This suggests that compounds inhibiting CDK5 and GSK3β together could be protective via multiple mechanisms.

Taken together, our results demonstrate that GSK3β and CDK5 have overlapping roles in inflammation-mediated neurodegeneration by mediating microtubule disassembly. As a result, it is necessary to inhibit both kinases simultaneously to rescue neuronal morphology, and we conclude that LDC8 is a promising compound for medicinal chemistry programs aimed at developing neuroprotective drugs.

EXPERIMENTAL PROCEDURES

Extended experimental and method details can be found in the Supplemental Information.

MN-Based Assays

Briefly, NSCs were cultured and differentiated into astrocytes. ESC-derived MNs were dissociated and plated on astrocytes. Thirty hours after addition of stress together with the test compound, the plates were analyzed using an Arrayscan VTI Live (Thermo Scientific). Differentiated human MNs were pre-treated with the respective compounds or DMSO controls 24 h before the stress was added. Next, the cells were stressed with DetaNO-containing medium in the presence of the respective compounds. Two days later, CellTiter-Glo (Promega) was performed.

Ethical Approval

All procedures performed in studies involving human participants were in accordance with the ethical standards of the institutional and/or national research committee and with the 1964 Helsinki Declaration and its later amendments or comparable ethical standards and approved by the Ethical Committee of the Technische Universität Dresden (EK45022009, EK393122012). The zebrafish experiments were carried out in strict accordance with European Union and German animal protection laws. All zebrafish larval experiments were performed using embryos that were 5 days post fertilization or less as stated in animal protection law (Tierschutz-Versuchstierverordnung – TierSchVersV §14). All zebrafish experiments in adult brains were carried out in accordance with the animal experimentation permits of the Landesdirektion Sachsen, Germany (TVV-35/2016 and TVV-52/2015).

SUPPLEMENTAL INFORMATION

Supplemental Information includes Supplemental Experimental Procedures, seven figures, and five tables and can be found with this article online at https://doi.org/10.1016/j.stemcr.2019.01.015.

AUTHOR CONTRIBUTIONS

L.R. and S.K. are joint first authors who contributed equally to this work; L.R., S.K., M. Baumann, M. Bickle, P.N., B.K., P.B., C.K., and J.S. designed the research; M. Bickle, L.R., S.K., P.R., M.G., H.C.A.D., S.M., G.Z., J.E., L.M., A.J., K.A., M.S., and P.B. performed the research; A.J. and H.C.A.D. contributed new reagents/analytic tools; and L.R. and J.S. wrote the paper.

ACKNOWLEDGMENTS

This work was financed by DFG Research Center (DFG FZT 111) and Cluster of Excellence (DFG EXC 168), the Max Planck Society, as well as the BMBF (01EK1606A). The Sterneckert lab is supported by the European Union's Horizon 2020 research and innovation program (643417) and the Bundesministerium für Bildung und Forschung (01ED1601B). This is an EU Joint Programme – Neurodegenerative Disease Research (JPND) project. The project is supported by the following funding organizations under the aegis of JPND—www.jpnd.eu: Germany, Bundesministerium für Bildung und Forschung; Israel, Ministry of Health; Italy, Ministero dell'Istruzione, dell'Università e della Ricerca; Sweden, Swedish Research Council; and Switzerland, Swiss National Science Foundation. KINOMEscan data were published (Fabian et al., 2005), and made publicly available, by the Harvard Medical School LINCS Center, which is funded by NIH grants U54 HG006097 and U54 HL127365. M.G. and L.M. are supported by the Hans and Ilse Breuer Stiftung. U.B.P. was supported by National Institutes of Health R01 (NS081303) and R21 grants (NS101661, NS100055, and NS098379), the Pennsylvania Tobacco Research grant, the Robert Packard Center for ALS Research at Johns Hopkins, The ALS Association, and the Muscular Dystrophy Association. C.K. was supported by the German Center for Neurodegenerative Diseases (DZNE) and Helmholtz Association (VH-NG-1021). We thank Tanya Levin for editing the manuscript. This work was additionally supported by the CRTD Light Microscopy, FACS, and *in vivo* testing facilities.

The Lead Discovery Center GmbH employs Susanne Kordes, Matthias Baumann, Sascha Menninger, Gunther Zischinsky, Jan Eickhoff, Peter Nussbaumer, and Bert Klebl.

Received: August 22, 2017
Revised: January 16, 2019
Accepted: January 17, 2019
Published: February 14, 2019

REFERENCES

Alonso, A.D., Grundke-Iqbal, I., Barra, H.S., and Iqbal, K. (1997). Abnormal phosphorylation of tau and the mechanism of Alzheimer neurofibrillary degeneration: sequestration of microtubule-associated proteins 1 and 2 and the disassembly of microtubules by the abnormal tau. Proc. Natl. Acad. Sci. U S A *94*, 298–303.

Bhattarai, P., Thomas, A.K., Cosacak, M.I., Papadimitriou, C., Mashkaryan, V., Zhang, Y., and Kizil, C. (2017a). Modeling amyloid-β42 toxicity and neurodegeneration in adult zebrafish brain. J. Vis. Exp. *128*. https://doi.org/10.3791/56014.

Bhattarai, P., Thomas, A.K., Papadimitriou, C., Cosacak, M.I., Mashkaryan, V., Froc, C., Kurth, T., Dahl, A., Zhang, Y., and Kizil, C. (2016). IL4/STAT6 signaling activates neural stem cell proliferation and neurogenesis upon Amyloid-β42 aggregation in adult zebrafish brain. Cell Rep. *17*, 941–948.

Bhattarai, P., Thomas, A.K., Zhang, Y., and Kizil, C. (2017b). The effects of aging on Amyloid-β42-induced neurodegeneration and regeneration in adult zebrafish brain. Neurogenesis (Austin) *4*, e1322666.

Chen, P., Lee, N.V., Hu, W., Xu, M., Ferre, R.A., Lam, H., Bergqvist, S., Solowiej, J., Diehl, W., He, Y.A., et al. (2016). Spectrum and degree of CDK drug interactions predicts clinical performance. Mol. Cancer Ther. *15*, 2273–2281.

de Munck, E., Palomo, V., Munoz-Saez, E., Perez, D.I., Gomez-Miguel, B., Solas, M.T., Gil, C., Martinez, A., and Arahuetes, R.M. (2016). Small GSK-3 inhibitor shows efficacy in a motor neuron disease murine model modulating autophagy. PLoS One *11*, e0162723.

Fabian, M.A., Biggs, W.H., 3rd, Treiber, D.K., Atteridge, C.E., Azimioara, M.D., Benedetti, M.G., Carter, T.A., Ciceri, P., Edeen, P.T., Floyd, M., et al. (2005). A small molecule-kinase interaction map for clinical kinase inhibitors. Nat. Biotechnol. *23*, 329–336.

Gordon, P.H., Moore, D.H., Miller, R.G., Florence, J.M., Verheijde, J.L., Doorish, C., Hilton, J.F., Spitalny, G.M., MacArthur, R.B., Mitsumoto, H., et al. (2007). Efficacy of minocycline in patients with amyotrophic lateral sclerosis: a phase III randomised trial. Lancet Neurol. *6*, 1045–1053.

Höing, S., Rudhard, Y., Reinhardt, P., Glatza, M., Stehling, M., Wu, G., Peiker, C., Bocker, A., Parga, J.A., Bunk, E., et al. (2012). Discovery of inhibitors of microglial neurotoxicity acting through multiple mechanisms using a stem-cell-based phenotypic assay. Cell Stem Cell *11*, 620–632.

Kang, S.H., Li, Y., Fukaya, M., Lorenzini, I., Cleveland, D.W., Ostrow, L.W., Rothstein, J.D., and Bergles, D.E. (2013). Degeneration and impaired regeneration of gray matter oligodendrocytes in amyotrophic lateral sclerosis. Nat. Neurosci. *16*, 571–579.

Kawauchi, T. (2014). Cdk5 regulates multiple cellular events in neural development, function and disease. Dev. Growth Differ. *56*, 335–348.

Knox, R.J., Friedlos, F., Jarman, M., and Roberts, J.J. (1988). A new cytotoxic, DNA interstrand crosslinking agent, 5-(aziridin-1-yl)-4-hydroxylamino-2-nitrobenzamide, is formed from 5-(aziridin-1-yl)-2,4-dinitrobenzamide (CB 1954) by a nitroreductase enzyme in Walker carcinoma cells. Biochem. Pharmacol. *37*, 4661–4669.

Koh, S.H., Kim, Y., Kim, H.Y., Hwang, S., Lee, C.H., and Kim, S.H. (2007). Inhibition of glycogen synthase kinase-3 suppresses the onset of symptoms and disease progression of G93A-SOD1 mouse model of ALS. Exp. Neurol. *205*, 336–346.

Kremer, A., Louis, J.V., Jaworski, T., and Van Leuven, F. (2011). GSK3 and Alzheimer's disease: facts and fiction. Front. Mol. Neurosci. *4*, 17.

Munzel, E.J., Schaefer, K., Obirei, B., Kremmer, E., Burton, E.A., Kuscha, V., Becker, C.G., Brosamle, C., Williams, A., and Becker, T. (2012). Claudin k is specifically expressed in cells that form myelin during development of the nervous system and regeneration of the optic nerve in adult zebrafish. Glia *60*, 253–270.

Nguyen, M.D., Lariviere, R.C., and Julien, J.P. (2001). Deregulation of Cdk5 in a mouse model of ALS: toxicity alleviated by perikaryal neurofilament inclusions. Neuron *30*, 135–147.

Reinhardt, P., Glatza, M., Hemmer, K., Tsytsyura, Y., Thiel, C.S., Hoing, S., Moritz, S., Parga, J.A., Wagner, L., Bruder, J.M., et al. (2013). Derivation and expansion using only small molecules of human neural progenitors for neurodegenerative disease modeling. PLoS One *8*, e59252.

Rideout, H.J., Wang, Q., Park, D.S., and Stefanis, L. (2003). Cyclin-dependent kinase activity is required for apoptotic death but not inclusion formation in cortical neurons after proteasomal inhibition. J. Neurosci. *23*, 1237–1245.

Shukla, V., Zheng, Y.L., Mishra, S.K., Amin, N.D., Steiner, J., Grant, P., Kesavapany, S., and Pant, H.C. (2013). A truncated peptide from p35, a Cdk5 activator, prevents Alzheimer's disease phenotypes in model mice. FASEB J. *27*, 174–186.

Smith, B.N., Ticozzi, N., Fallini, C., Gkazi, A.S., Topp, S., Kenna, K.P., Scotter, E.L., Kost, J., Keagle, P., Miller, J.W., et al. (2014). Exome-wide rare variant analysis identifies TUBA4A mutations associated with familial ALS. Neuron *84*, 324–331.

Turner, M.R., Cagnin, A., Turkheimer, F.E., Miller, C.C., Shaw, C.E., Brooks, D.J., Leigh, P.N., and Banati, R.B. (2004). Evidence of widespread cerebral microglial activation in amyotrophic lateral sclerosis: an [11C](R)-PK11195 positron emission tomography study. Neurobiol. Dis. *15*, 601–609.

Vera, J.H., Ridha, B., Gilleece, Y., Amlani, A., Thorburn, P., and Dizdarevic, S. (2017). PET brain imaging in HIV-associated neurocognitive disorders (HAND) in the era of combination antiretroviral therapy. Eur. J. Nucl. Med. Mol. Imaging *44*, 895–902.

Xu, X., Lei, Y., Luo, J., Wang, J., Zhang, S., Yang, X.J., Sun, M., Nuwaysir, E., Fan, G., Zhao, J., et al. (2013). Prevention of beta-amyloid induced toxicity in human iPS cell-derived neurons by inhibition of Cyclin-dependent kinases and associated cell cycle events. Stem Cell Res. *10*, 213–227.

Zheng, Y.L., Amin, N.D., Hu, Y.F., Rudrabhatla, P., Shukla, V., Kanungo, J., Kesavapany, S., Grant, P., Albers, W., and Pant, H.C. (2010). A 24-residue peptide (p5), derived from p35, the Cdk5 neuronal activator, specifically inhibits Cdk5-p25 hyperactivity and tau hyperphosphorylation. J. Biol. Chem. *285*, 34202–34212.